J|A|C|S COMMUNICATIONS

Published on Web 01/21/2009

Formation of Self-Assembled Polyelectrolyte Multilayer Nanodots by Scanning Probe Microscopy

Geunhee Lee, Young-Han Shin, and Jong Yeog Son*

Department of Materials Science and Engineering, Pohang University of Science and Technology (POSTECH), Pohang 790-784, Korea

Received August 27, 2008; E-mail: sonjyson@postech.ac.kr

Polyelectrolyte multilayer films formed by alternating stacks of oppositely charged polyelectrolyte monolayers in a layer-by-layer manner[1−4] have been attractively researched for the applications of integrated optics, plastic electronics, organic light-emitting diodes, sensors, and optical memory devices owing to their advantages of well-defined thickness, composition, and surface properties.[5,6] The electrostatic interaction between the opposite charges of the adjacent polyelectrolyte layers was believed to be the main driving force for the multilayer formation.[7]

Meanwhile, scanning probe microscopy (SPM) is a powerful tool for analyzing surface in nanoscale and atomic scale.[8−11] It is possible to move atoms on the surface of films and measure the surface potential by SPM techniques including atomic force microscopy (AFM) and Kelvin probe force microscopy (KFM). In addition, the force involved in interactions between atoms can be used to modify surface morphology like lithography.[9,11] These capabilities can be used for many applications like nanolithography and data storage.[10,12] Thus, surface topography and potential measurement techniques by SPM enable the writing and reading of charges on the surface of insulators as a charge lithography method in nanoscale.[12] Here, we suggest a promising way to pattern polyelectrolyte multilayer films using the SPM lithography technique for various nanodevice applications.

In this study, we demonstrate that patterned nanodots can be obtained from alternatively self-assembled polyelectrolytes which consist of poly(acrylic acid) (PAA) and poly(allylamine hydrochloride) (PAH) by using AFM (Seiko SPA400).[13] The patterned nanodots exhibited a well-quantized increase in thickness depending on the number of PAA and PAH layers with the varying surface potential following the type of the top layer polyelectrolyte.

A schematic drawing of writing a nanodot with self-assembled polyelectrolyte multilayers by AFM is depicted in Figure 1. At first, we form a 100 nm thick SiO_2 film as a substrate for surface charge patterns. The SiO_2 film is prepared by thermal oxidation of a Si substrate for 2 h at 1000 °C.[14] After that, we charge an electron charge nanobit with 50 nm in diameter on the SiO_2 film by a bias voltage of 10 V between the Si substrate and the gold coated Si_3N_4 AFM cantilever. On the electron nanobit we exactly attach a PAH monolayer, preserving the shape of the electron nanobit. This PAH monolayer forms a nanodot in a uniform thickness as high as a PAH monolayer thickness with a positive surface potential resulting from the positive charge (NH_3^+) in PAH. Following that, we attach a PAA monolayer on the PAH monolayer nanodot by using the electrostatic interaction between the PAA and PAH monolayers. The attached PAA monolayer increases the nanodot thickness as high as the uniform thickness of a PAA monolayer with a negative surface potential resulting from the negative charge (COO^-) in PAA. Finally, we can attach an additional PAH monolayer on the preformed PAA/PAH nanodot, in which the thickness of the nanodot also increases as high as the thickness of a PAH monolayer

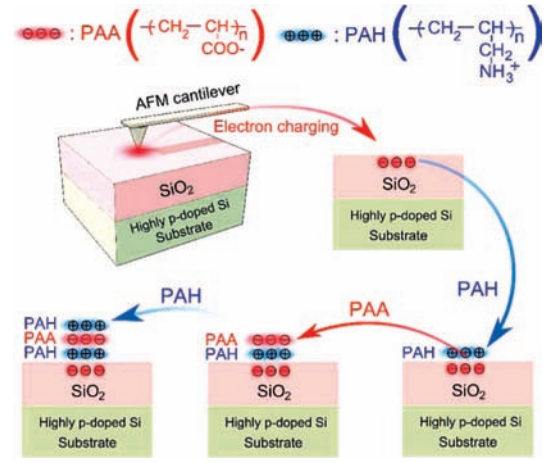

Figure 1. Schematic of writing a nanodot with self-assembled polyelectrolyte multilayers on the confined area of insulating SiO_2 by charging with AFM.

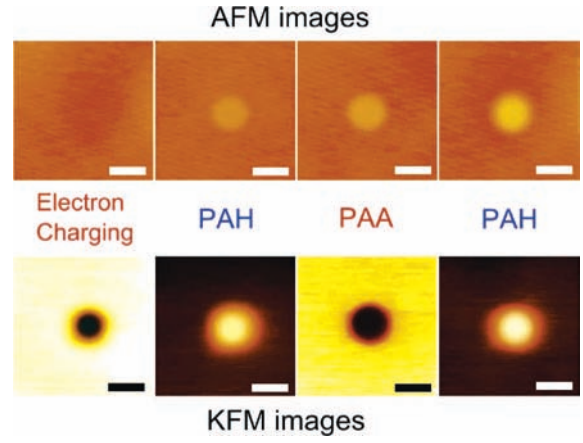

Figure 2. The AFM and KFM images of the electron charge nanobit and the PAH monolayer, PAA/PAH multilayer, and PAH/PAA/PAH multilayer nanodots. The scale bar in each panel corresponds to 50 nm.

with a positive surface potential. Consequently, we can form a nanodot which has desirable morphology and thicknesses with alternating PAA and PAH monolayers and control surface charge types in nanoscale.

In this experiment, the acidity of PAA and PAH solutions was set to pH 6, which gave a well-known monolayer thickness of about 0.5 nm.[15] During the experimental steps, we simultaneously measured AFM topographies and KFM potentials (Figure 2) in nitrogen atmosphere.[11] There was no topographical change in the electron charge nanobit compared to the bare surface of the SiO_2 film as shown in the AFM image, while the electron charge nanobit

10.1021/ja806795a CCC: $40.75

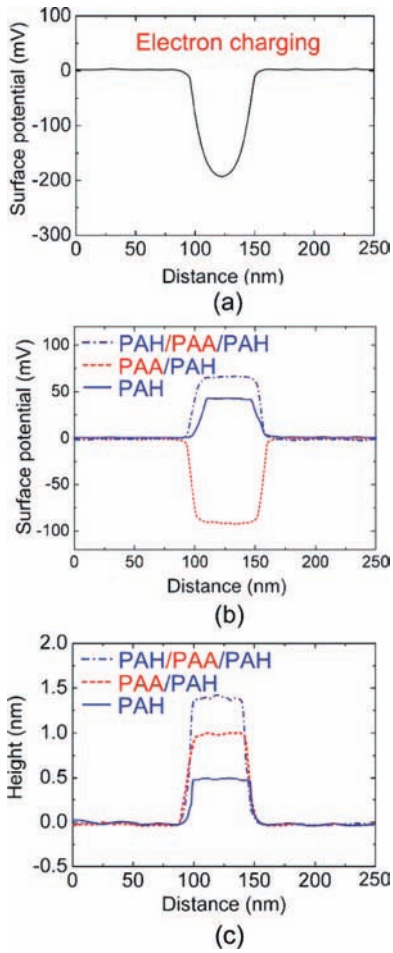

Figure 3. AFM and KFM profiles of an electron charge nanobit and multilayer nanodots: (a) KFM potential of the electron charge nanobit; (b) KFM surface potentials of the PAH, PAA/PAH, and PAH/PAA/PAH nanodots; (c) AFM topographies of the PAH, PAA/PAH, and PAH/PAA/PAH nanodots.

with a diameter of about 50 nm was clearly observed in the KFM image. However, we observed the topographical changes in the multilayer nanodots (e.g., the PAH monolayer, PAA/PAH multilayer, and PAH/PAA/PAH multilayer nanodots) with the same diameter as the electron charge nanobit in the AFM images. This means that the PAA or PAH monolayers are well attached along the shape and size of the charge nanobit on the SiO_2 surface as well as the PAA and PAH multilayer nanodots. In addition, there is possible existence of counterions (Na^+, H^+, OH^-, and Cl^- ions) on the surface of polyelectrolytes. However, we did not observe a significant change in surface potentials influenced by these counterions. Consequently, the KFM images in Figure 2 well reflect the polarities of the three nanodots depending on the polyelectrolyte type of the top layer.

To check the variations of the topography and the surface potential for the four states, we present line profiles which pass over the center of the nanobit and nanodots for the AFM and KFM images. The electron charge nanobit exhibits the surface potential of about −200 mV without any topographical change (Figure 3a). The PAH monolayer, PAA/PAH multilayer, and PAH/PAA/PAH multilayer nanodots show the bipolarity of the surface potential depending on the type of the top layer (Figure 3b). This means that the surface potentials are easily reversible to positive or negative states by choosing the type of the top polyelectrolyte layer. It is notable that these polyelectrolyte multilayer nanodots, which were formed just on the charged area, exhibit the controllable thicknesses that proportionally increase to the total number of monolayers with a uniform thickness of about 0.5 nm as shown in Figure 3c. Generally, polyelectrolyte multilayers have an interdigitated nature.[2] In particular, we obtained a nearly discrete increase in thickness for three polyelectrolyte multilayer nanodots, which is probably due to the immediate observation of AFM and KFM images after forming each nanodot.

In summary, the patternable formation of self-assembled polyelectrolyte multilayer nanodots was studied using AFM and KFM. The nanodots were grown in a layer-by-layer manner exactly on the charged area. Their thicknesses proportionally increased to the total number of monolayers with a uniform thickness of about 0.5 nm. We suggest that the SPM lithography technique is a promising way to pattern polyelectrolyte multilayer nanodots in which size is controllable with accuracy in nanoscale.

Acknowledgment. This work was supported by the Brain Korea 21 Project 2008.

References

(1) Lvov, Y.; Decher, G.; Sukhorukov, G. *Macromolecules* **1993**, *26*, 5396–5399.
(2) Radeva, T.; Grozeva, M. *J. Colloid Interface Sci.* **2005**, *287*, 415–421.
(3) Wu, A.; Yoo, D.; Lee, J. K.; Rubner, M. F. *J. Am. Chem. Soc.* **1999**, *121*, 4883–4891.
(4) Yamada, T.; Shiratori, S. *Mol. Cryst. Liq. Cryst.* **2001**, *370*, 289–292.
(5) Decher, G. *Science* **1997**, *277*, 1232–1237.
(6) Hammond, P. T. *Adv. Mater.* **2004**, *16*, 1271–1293.
(7) Dubas, S. T.; Schlenoff, J. B. *Macromolecules* **1999**, *32*, 8153–8160.
(8) Binnig, G.; Rohrer, H.; Gerber, C.; Weibel, E. *Phys. Rev. Lett.* **1982**, *49*, 57.
(9) Binnig, G.; Quate, C. F.; Gerber, C. *Phys. Rev. Lett.* **1986**, *56*, 930.
(10) Majumdar, A.; Oden, P. I.; Carrejo, J. P.; Nagahara, L. A.; Graham, J. J.; Alexander, J. *Appl. Phys. Lett.* **1992**, *61*, 2293–2295.
(11) Jacobs, H. O.; Knapp, H. F.; Stemmer, A. *Rev. Sci. Instrum.* **1999**, *70*, 1756–1760.
(12) Tzeng, S.-D.; Lin, K.-J.; Hu, J.-C.; Chen, L.-J.; Gwo, S. *Adv. Mater.* **2006**, *18*, 1147–1151.
(13) Yoo, D.; Shiratori, S. S.; Rubner, M. F. *Macromolecules* **1998**, *31*, 4309–4318.
(14) Deal, B. E.; Grove, A. S. *J. Appl. Phys.* **1965**, *36*, 3770–3778.
(15) Wang, T. C.; Chen, B.; Rubner, M. F.; Cohen, R. E. *Langmuir* **2001**, *17*, 6610–6615.

JA806795A